Neuro-Oncology
19(5), 699–709, 2017 | doi:10.1093/neuonc/now254 | Advance Access date 14 November 2016



# Targeted next-generation sequencing of pediatric neuro-oncology patients improves diagnosis, identifies pathogenic germline mutations, and directs targeted therapy

**Cassie N. Kline,* Nancy M. Joseph,* James P. Grenert, Jessica van Ziffle, Eric Talevich, Courtney Onodera, Mariam Aboian, Soonmee Cha, David R. Raleigh, Steve Braunstein, Joseph Torkildson, David Samuel, Michelle Bloomer, Alejandra G. de Alba Campomanes, Anuradha Banerjee, Nicholas Butowski, Corey Raffel, Tarik Tihan, Andrew W. Bollen, Joanna J. Phillips, W. Michael Korn, Iwei Yeh, Boris C. Bastian, Nalin Gupta, Sabine Mueller, Arie Perry, Theodore Nicolaides, and David A. Solomon**

*Division of Pediatric Hematology/Oncology, Department of Pediatrics, University of California San Francisco (UCSF), San Francisco, California (C.N.K., A.B., S.M., T.N.); Department of Pathology, UCSF, San Francisco, California (N.M.J., J.P.G., J.V.Z., T.T., A.W.B., J.J.P., I.Y., B.C.B., A.P., D.A.S.); Clinical Cancer Genomics Laboratory, UCSF, San Francisco, California (N.M.J., J.P.G., J.V.Z., E.T., C.O., I.Y., B.C.B., D.A.S.); Department of Radiology, UCSF, San Francisco, California (M.A., S.C.); Department of Neurological Surgery, UCSF, San Francisco, California (S.C., A.B., C.R., J.J.P., N.G., S.M., A.P., T.N.); Department of Radiation Oncology, UCSF, San Francisco, California (D.R.R., S.B.); Division of Pediatric Hematology/Oncology, UCSF Benioff Children's Hospital Oakland, Oakland, California (J.T.); Division of Pediatric Hematology/Oncology, Valley Children's Hospital, Madera, California (D.S.); Department of Ophthalmology, UCSF, San Francisco, California (M.B., A.A.C.); Division of Neuro-Oncology, Department of Neurological Surgery, UCSF, San Francisco, California (N.B.); Divisions of Gastroenterology and Medical Oncology, Department of Medicine, UCSF, San Francisco, California (M.K.)*

**Corresponding Authors:** Theodore Nicolaides, MD, Division of Pediatric Hematology/Oncology, Department of Pediatrics, University of California, San Francisco, 550 16th Street, Box 0434, San Francisco, CA 94143 (theodore.nicolaides@ucsf.edu). David A. Solomon, MD, PhD, Division of Neuropathology, Department of Pathology, University of California, San Francisco, Health Sciences West 451, 513 Parnassus Ave, San Francisco, CA 94143 (david.solomon@ucsf.edu).

*These authors contributed equally to this study.

**Abstract**

**Background.** Molecular profiling is revolutionizing cancer diagnostics and leading to personalized therapeutic approaches. Herein we describe our clinical experience performing targeted sequencing for 31 pediatric neuro-oncology patients.

**Methods.** We sequenced 510 cancer-associated genes from tumor and peripheral blood to identify germline and somatic mutations, structural variants, and copy number changes.

**Results.** Genomic profiling was performed on 31 patients with tumors including 11 high-grade gliomas, 8 medulloblastomas, 6 low-grade gliomas, 1 embryonal tumor with multilayered rosettes, 1 pineoblastoma, 1 uveal ganglioneuroma, 1 choroid plexus carcinoma, 1 chordoma, and 1 high-grade neuroepithelial tumor. In 25 cases (81%), results impacted patient management by: (i) clarifying diagnosis, (ii) identifying pathogenic germline mutations, or (iii) detecting potentially targetable alterations. The pathologic diagnosis was amended after genomic profiling for 6 patients (19%), including a high-grade glioma to pilocytic astrocytoma, medulloblastoma to pineoblastoma, ependymoma to high-grade glioma, and medulloblastoma to CNS high-grade neuroepithelial tumor with *BCOR* alteration. Multiple patients had pathogenic germline mutations, many of which were previously unsuspected. Potentially targetable alterations were identified in 19 patients (61%). Additionally, novel likely pathogenic alterations were identified in 3 cases: an in-frame *RAF1* fusion in a *BRAF* wild-type pleomorphic xanthoastrocytoma, an inactivating *ASXL1* mutation in a histone H3

wild-type diffuse pontine glioma, and an in-frame deletion within exon 2 of *MAP2K1* in a low-grade astrocytic neoplasm.

**Conclusions.** Our experience demonstrates the significant impact of molecular profiling on diagnosis and treatment of pediatric brain tumors and confirms its feasibility for use at the time of diagnosis or recurrence.

**Key words**

molecular profiling | next-generation sequencing | pediatric brain tumors | personalized therapy | targeted therapeutics

## Importance of the study

The following paper details our institutional experience performing targeted somatic and germline sequencing in pediatric neuro-oncology patients. We highlight the feasibility of genomic profiling in both the primary and recurrent disease setting and demonstrate the significant impact this testing is having on confirming pathologic diagnosis, identifying germline mutations, and elucidating potentially targetable molecular alterations. We anticipate that this testing will serve as the basis for future clinical trials of personalized targeted therapy, leading to improved outcomes for children with brain tumors.

Brain tumors are the most common pediatric solid malignancy and the second most common pediatric cancer, yet they exhibit some of the most stagnant survival curves. Diffuse intrinsic pontine gliomas (DIPGs) and supratentorial high-grade gliomas are only 2 examples that have shown little to no improvement after years of varying therapeutic approaches.[1] Poor outcomes combined with long-term sequelae following radiation and/or cytotoxic chemotherapy have led investigators and providers to search for better prognostic indicators, predictors of response, and novel treatment strategies. Accordingly, a movement towards molecularly based diagnostic and treatment approaches has begun in recent years with a direction seemingly headed to personalized therapy for each patient.[2]

High-throughput sequencing has made possible the ability to molecularly profile patients and tumors at time of diagnosis, thus leading to cancer diagnoses and treatment beyond histopathology and traditional, standard-of-care therapies.[3,4] Genomic profiling has been carried out across a multitude of pediatric CNS tumors, revealing targetable driver mutations and molecularly distinct tumor subtypes.[5] Certainly, medulloblastoma is a prime example of how molecular profiling has improved risk stratification, prognostic prediction, and focused treatment strategies. As recently as 2007, medulloblastoma was classified by histology alone as classic, anaplastic, large cell, desmoplastic/nodular, or extensive nodularity. Genetic profiling has since led to a restructuring of medulloblastoma classification and by 2012, these tumors are now subclassified according to the molecular pathways that drive tumor development—Wnt pathway activated; SHH pathway activated; Group 3; and Group 4.[6] Treatment approaches including recent clinical trials are now based on molecular subtypes, as this new system appears to better predict clinical outcomes than histology alone.[7] Support for genetic profiling in pediatric cancer patients has been further bolstered by recent reports of a high frequency of pathogenic germline mutations in several pediatric neoplasms, particularly brain tumors.[8]

With these advancements, institutions are working to incorporate genomic profiling into routine patient care to improve diagnostic accuracy, better predict outcome, and personalize therapy.[3,4] Our medical center is implementing these techniques in the pediatric neuro-oncology population and now has a year of practice in doing so. Herein we describe our experience using next-generation sequencing to diagnose and treat children with a variety of brain tumors and document how genomic profiling has significantly augmented the comprehensive nature of our treatment strategy.

## Methods

The 31 patients selected for sequencing represented a subset of the 100+ pediatric neuro-oncology patients who were either treated at UCSF Medical Center or seen for second opinion regarding treatment options during the study period. Cases selected for sequencing were chosen according to: (i) diagnostic uncertainty based on histology alone, (ii) diagnoses without successful standard-of-care therapeutic options, and (iii) tumors that progressed through prior therapies. Informed consent was obtained prior to genetic sequencing. This study was approved by the UCSF institutional review board.

Genomic DNA was extracted from peripheral blood and tumor tissue micro-dissected from formalin-fixed, paraffin-embedded blocks. Capture-based next-generation sequencing (NGS) was performed at the UCSF Clinical Cancer Genomics Laboratory, using an assay targeting the coding regions of 510 cancer-related genes, *TERT* promoter, select introns from 40 genes (for detection of gene fusions and other structural variants), and intergenic regions at regular intervals along each chromosome (for

chromosomal copy number assessment), altogether with a total sequencing footprint of 2.8 Mb (UCSF500 Cancer Gene Panel, Supplementary Fig. 1). Sequencing libraries were prepared from genomic DNA with target enrichment performed by hybrid capture using a custom oligonucleotide library. Sequencing was performed on an Illumina HiSeq 2500. Duplicate sequencing reads were removed computationally to allow for accurate allele frequency determination and copy number estimates. The analysis was based on the human reference sequence UCSC build hg19 (NCBI build 37), using the following software packages: BWA, Samtools, Picard tools, GATK, CNVkit, Pindel, SATK, Annovar, Freebayes, Delly, and Nexus Copy Number (see Supplementary References 1–8). Single nucleotide variants and small insertions/deletions (indels) were visualized and verified using Integrated Genome Viewer. For samples with at least 25% tumor, >200× coverage for the tumor sample, and >100× coverage for the normal sample, the sensitivity is 99% and 83% and the specificity is 98% and 71% for fully clonal single nucleotide variants and small indels, respectively. Sensitivity of detection of copy number changes is >98% for samples with high tumor content. Large insertions, deletions, and gene rearrangements may be detected but have only been individually validated for select examples.

Molecular pathologists with specialization in neuropathology and brain tumor genetics organized results into formal reports, which detailed somatic and germline alterations as well as association with any known tumor predisposition syndromes, diagnostic or prognostic implications, and potential targeted therapies (example in Supplementary Fig. 2). Results were discussed at weekly multidisciplinary molecular tumor boards that included surgical and molecular pathologists together with oncologists, surgeons, and radiation oncologists from a wide variety of specialties.

## Results

Between June 2015 and May 2016, genomic profiling was performed on 31 pediatric neuro-oncology patients (Table 1). Nineteen patients (61%) were male. Patient age ranged from 13 months to 19 years (median 9.6 y). Tumors included 11 high-grade gliomas, 8 medulloblastomas, 6 low-grade gliomas, 1 embryonal tumor with multilayered rosettes, 1 pineoblastoma, 1 uveal ganglioneuroma, 1 choroid plexus carcinoma, 1 metastatic chordoma, and 1 high-grade neuroepithelial tumor. Turn-around time from receipt of tumor tissue and peripheral blood to completion of formal report and discussion at molecular tumor board ranged from 14 to 21 days. The list of pathogenic alterations identified in the germline and tumor of each patient is presented in Table 1.

### Clarification of Pathologic Diagnoses

The initial pathologic diagnosis was amended in 6 of 31 patients (19%) based on results of genomic profiling. Four of these cases are described below and illustrated in Fig. 1 to demonstrate how integrating the results of this genomic profiling with histologic and radiographic findings has improved diagnostic classification.

Patient 28 is a 9-year-old girl with a peripherally enhancing tectal mass with associated T2/ fluid attenuated inversion recovery (FLAIR) hyperintensity extending into bilateral thalami (Fig. 1A–B). Biopsy revealed an astrocytic neoplasm with a few Rosenthal fibers and no high-grade histologic features (Fig. 1C). Immunohistochemical staining revealed intact expression of ATRX and no positivity with antibodies against BRAF-V600E, isocitrate dehydrogenase 1 (IDH1)-R132H, or histone H3-K27M mutant proteins. While the pathology was classified as an astrocytoma of indeterminate grade, imaging was thought to be more suggestive of a high-grade, infiltrative tumor. The patient was treated with focal irradiation and was receiving maintenance chemotherapy with temozolomide when genomic profiling was performed to clarify the diagnosis and identify therapeutic targets. Targeted sequencing revealed *KIAA1549-BRAF* gene fusion with no other genetic alterations. The pathologic diagnosis was amended to pilocytic astrocytoma, World Health Organization (WHO) grade I, and treatment with temozolomide was discontinued.

Patient 10 is an 18-month-old boy with progressive weakness and a solid, avidly enhancing mass centered in the midline of the posterior fossa (Fig. 1D). Histology revealed a primitive small blue cell tumor with high mitotic index (Fig. 1E–F), and an initial diagnosis of medulloblastoma, WHO grade IV, was rendered given presumed origin from the cerebellar vermis. Subsequent genomic profiling revealed somatic mutations including *DICER1* frameshift and hotspot missense mutations, *ARID1A* frameshift mutation, and *KDM5C* missense mutation. No genetic alterations typical of medulloblastoma were identified. Based on this genomic profiling and recurrent *DICER1* mutations that are known to be present in pineoblastoma,[9] the preoperative imaging was re-reviewed showing an anatomic location superior to typical medulloblastoma cases, lack of visualization of the pineal gland, and mass effect on the subjacent cerebellar vermis. The diagnosis was subsequently amended to pineoblastoma, WHO grade IV.[10]

Patient 22 is an 11-year-old boy with a complex, solid, and cystic mass in the suprasellar region with dissemination along the right Sylvian fissure and spinal cord (Fig. 1G). Biopsy of a spinal cord metastasis demonstrated a mitotically active glial neoplasm with anuclear perivascular zones containing dense glial processes resembling perivascular pseudorosettes, initially interpreted as ependymoma by the referring pathologist (Fig. 1H). However, diffuse, strong immunostaining for oligodendrocyte transcription factor (OLIG2) was present in tumor cells (Fig. 1I), arguing against ependymoma. Genomic profiling revealed an activating missense mutation within the kinase domain of *FGFR1* (p.K565E), which has been recurrently found in pilocytic astrocytomas and other pediatric low-grade gliomas.[11,12] A molecularly integrated diagnosis of high-grade glioma with *FGFR1* mutation was made, with one likely possibility being anaplastic transformation and dissemination from a pilocytic astrocytoma originating in the suprasellar region.

Patient 11 is a 4-year-old girl who was found to have a large, well-circumscribed mass in the right cerebellar hemisphere (Fig. 1J). Resection of the tumor demonstrated a solid, non-infiltrative malignant neoplasm composed of numerous

**Table 1** Pediatric neuro-oncology patients who underwent genomic profiling of tumor and peripheral blood

| Patient | Sex | Age | Site | Pathologic Diagnosis | Germline | Somatic |
|---|---|---|---|---|---|---|
| 1 | M | 10 | Posterior fossa | Medulloblastoma, classic | None | None |
| 2 | M | 6 | Posterior fossa | Medulloblastoma, nodular/ desmoplastic | None | None |
| 3 | F | 2 | Posterior fossa | Medulloblastoma, nodular/ desmoplastic | BRCA2 fs + fs (biallelic) | PTCH1 splice, GLI2 amp |
| 4 | M | 5 | Posterior fossa | Medulloblastoma, large cell/ anaplastic | PALB2 non | PALB2 LOH |
| 5 | M | 2 | Posterior fossa | Medulloblastoma, nodular/ desmoplastic | SUFU fs | SUFU LOH, KDM6A non |
| 6 | F | 6 | Posterior fossa | Medulloblastoma, nodular/ non-desmoplastic | None | None |
| 7 | M | 9 | Posterior fossa | Medulloblastoma, nodular/ desmoplastic | TP53 sub | TP53 LOH, PTCH1 non, PTEN del |
| 8 | M | 8 | Posterior fossa | Medulloblastoma, classic | None | None |
| 9 | M | 3 | L parietal lobe | Choroid plexus carcinoma | TP53 sub, MSH6 fs | TP53 LOH |
| 10 | M | 1 | Pineal region | Pineoblastoma[1] | None | DICER1 sub + fs, ARID1A fs, KDM5C sub |
| 11 | F | 4 | Posterior fossa | High-grade neuroepithelial tumor[2] | None | BCOR exon 15 internal tandem dup |
| 12 | F | 1 | Pons | Embryonal tumor with mutlilayered rosettes | None | C19MC amp |
| 13 | M | 4 | Spinal cord, thoracic | Glioblastoma | MUTYH non | H3F3A K27M, ACVR1 sub, PIK3CA sub |
| 14 | F | 2 | R frontal lobe | Glioblastoma | None | hypermutated including TP53, NF1, SETD2, ATRX, KDM6A, PTPN11, BRCA2 |
| | | 3 | L parietal lobe | Glioblastoma[3] | None | hypermutated including TP53, NF1, SETD2, ATRX, PTEN, ARID1A, POLE |
| 15 | F | 17 | R frontal lobe | Glioblastoma | None | hypermutated including MSH6 fs, ATRX fs, TP53 sub, CDKN2A del, SETD2 fs, PDGFRA amp |
| 16 | M | 11 | R thalamus | Glioblastoma | None | H3F3A K27M, TP53 sub, BCORL1 non |
| 17 | F | 10 | L thalamus | Glioblastoma | None | AKT3 amp, CDK4 amp, MDM2 amp, PDGFRA amp + sub |
| 18 | M | 10 | R parietal lobe | Glioblastoma | PMS2 non + del | hypermutated including MSH6 non, TP53 sub, PTEN sub, SETD2 non, NF1 non, ATRX fs |
| 19 | F | 7 | L temporal lobe | High-grade infiltrative astrocytoma | TP53 sub | TP53 LOH, PIK3CA sub |
| 20 | M | 15 | Pons | High-grade infiltrative astrocytoma | MUTYH splice | MUTYH LOH, CDKN2A del, PDGFRA sub |
| 21 | M | 12 | Pons | Infiltrative astrocytoma, post-radiation therapy | None | PIK3CA sub, TP53 sub, ASXL1 non |
| 22 | M | 11 | Suprasellar w/ dissemination | High-grade glioma[4] | None | FGFR1 sub |
| 23 | M | 12 | L temporal lobe | Diffuse astrocytoma | ERCC2 splice | IDH1 R132H, TP53 sub + fs |
| 24 | F | 14 | L frontal lobe | Diffuse astrocytoma, recurrent[5] | None | IDH1 R132H, TP53 fs |
| 25 | M | 12 | L temporal lobe | Low-grade astrocytic neoplasm | None | MAP2K1 exon 2 small in-frame del |
| 26 | M | 2 | R frontal lobe | Oligodendroglioma | None | FGFR1 kinase domain dup |
| 27 | F | 14 | Posterior fossa w/ dissemination | Pilocytic astrocytoma | None | KIAA1549-BRAF fusion |
| 28 | F | 9 | Tectum/Midbrain | Pilocytic astrocytoma[6] | None | KIAA1549-BRAF fusion |

**Table 1** Continued

| Patient | Sex | Age | Site | Pathologic Diagnosis | Germline | Somatic |
|---|---|---|---|---|---|---|
| 29 | M | 19 | L parietal lobe | Anaplastic plemorphic xanthoastrocytoma, recurrent | None | ATG7-RAF1 fusion, CDKN2A del |
| 30 | F | 5 | R globe | Uveal ganglioneuroma | PTEN non | PTEN LOH |
| 31 | M | 11 | Scalp metastasis from clival tumor | Poorly differentiated chordoma, metastatic | None | SMARCB1 del |

**Abbreviations:** sub, missense mutation; non, nonsense mutation; fs, frameshift mutation; splice, splice site mutation; LOH, loss of heterozygosity; del, homozygous deletion; amp, focal high level amplification; dup, duplication.
1. Diagnosis changed following genomic profiling from medulloblastoma to pineoblastoma.
2. Diagnosis changed following genomic profiling from anaplastic medulloblastoma to CNS high-grade neuroepithelial tumor with BCOR alteration.
3. Diagnosis changed following genomic profiling from recurrent glioblastoma to a second de novo glioblastoma.
4. Diagnosis changed following genomic profiling from ependymoma to high-grade glioma.
5. Diagnosis changed following genomic profiling from oligodendroglioma to diffuse astrocytoma.
6. Diagnosis changed following genomic profiling from astrocytoma consistent with high grade based on imaging features to pilocytic astrocytoma.

rosettes containing central areas of eosinophilic cell processes with high mitotic index and foci of necrosis, initially interpreted as anaplastic medulloblastoma by the referring pathologist (Fig. 1K–L). However, the tumor was negative for synaptophysin and neurofilament, with patchy OLIG2 staining noted, arguing against a diagnosis of medulloblastoma. Genomic profiling revealed a somatic internal tandem duplication within exon 15 of *BCOR* (Supplementary Fig. 3), identical to that identified in the new molecular subtype of pediatric brain tumors entitled "CNS high-grade neuroepithelial tumor with BCOR alteration."[13] Thus, a molecularly integrated diagnosis of CNS high-grade neuroepithelial tumor with *BCOR* exon 15 internal tandem duplication was made.

## Identification of Pathogenic Germline Mutations

Eleven patients (35%) had pathogenic alterations identified in the germline, which were previously unsuspected in all but one medulloblastoma patient. While several of these germline mutations represent known associations in pediatric neuro-oncology such as *TP53* mutation with choroid plexus carcinoma and *SUFU* mutation with medulloblastoma, multiple novel pathogenic germline alterations were discovered. These included *MUTYH* mutations in 2 children with diffuse midline gliomas, monoallelic *PALB2* mutation in a child with medulloblastoma, and *PTEN* mutation in a child with uveal ganglioneuroma. Additional clinical details on the 11 patients with pathogenic germline alterations are presented in Table 2. Cases with novel pathogenic germline alterations are highlighted below and illustrated in Fig. 2, with additional select cases illustrated in Supplementary Fig. 4.

Two children with diffuse midline gliomas exhibited inactivating germline *MUTYH* mutations, which we recently reported and are briefly summarized here.[14] Patient 13 is a 4-year-old boy with a subtotally resected glioblastoma from the thoracic spinal cord. Genomic profiling revealed a germline *MUTYH* nonsense mutation without detectable alteration of the remaining wild-type allele in the germline or tumor. Somatic mutations in the tumor included *H3F3A* p.K27M, *ACVR1* p.G328E, and *PIK3CA* p.Q546K, which is the first example of an activating *ACVR1* mutation occurring in a glioma arising outside of the pons. Patient 20 is a 15-year-old boy with a history of medulloblastoma at age 5 who was then found to have an expansile mass in the pons diagnosed as high-grade infiltrative astrocytoma, histone H3-K27 wild-type, on stereotactic biopsy. Genomic profiling revealed a germline *MUTYH* splice site mutation with loss of the remaining wild-type allele in the tumor. Also found in the tumor was homozygous deletion of *CDKN2A* and activating missense mutation in *PDGFRA*.

Patient 4 is a 5-year-old boy with a family history of breast cancer in both maternal and paternal lineages who was found to have an enhancing multinodular mass centered in the fourth ventricle and left cerebellar hemisphere (Fig. 2A). He underwent resection that demonstrated medulloblastoma with diffuse anaplasia and large cell histologic features (Fig. 2B–C). Genomic profiling was performed that identified a germline *PALB2* nonsense mutation with loss of heterozygosity in the tumor, as well as numerous chromosomal copy number changes typical of tumors with defects in homologous recombination, including changes common to Group 3 medulloblastomas such as losses of 10q and 17p and gains of 1q and 17q (Fig. 2D). While biallelic germline *PALB2* mutations are causative of Fanconi anemia and increased susceptibility to medulloblastoma and other pediatric malignancies, monoallelic *PALB2* mutation in the germline has only been previously recognized to increase risk of breast, ovarian, and pancreatic carcinomas in adults.[15]

Patient 30 is a 5-year-old girl with a history of macrocephaly and autism who underwent enucleation of a blind, painful eye after 2 years of unilateral refractory glaucoma of uncertain etiology. MR imaging of the orbits showed diffuse thickening of the uveal tract in the right globe (Fig. 2E). Pathology revealed expansion of the entire uveal tract, including the ciliary body and iris by an S-100 immunopositive spindle cell neoplasm containing scattered large dysmorphic ganglion cells, diagnostic of uveal ganglioneuroma (Fig. 2F–H). Genomic profiling revealed a germline *PTEN* nonsense mutation accompanied by loss of heterozygosity in the tumor, indicative of Cowden syndrome. A cavernous malformation in the left occipital lobe (Fig. 2I) and an arteriovenous malformation in the subcutis of the upper extremity and foot are also present in the patient. Family history is

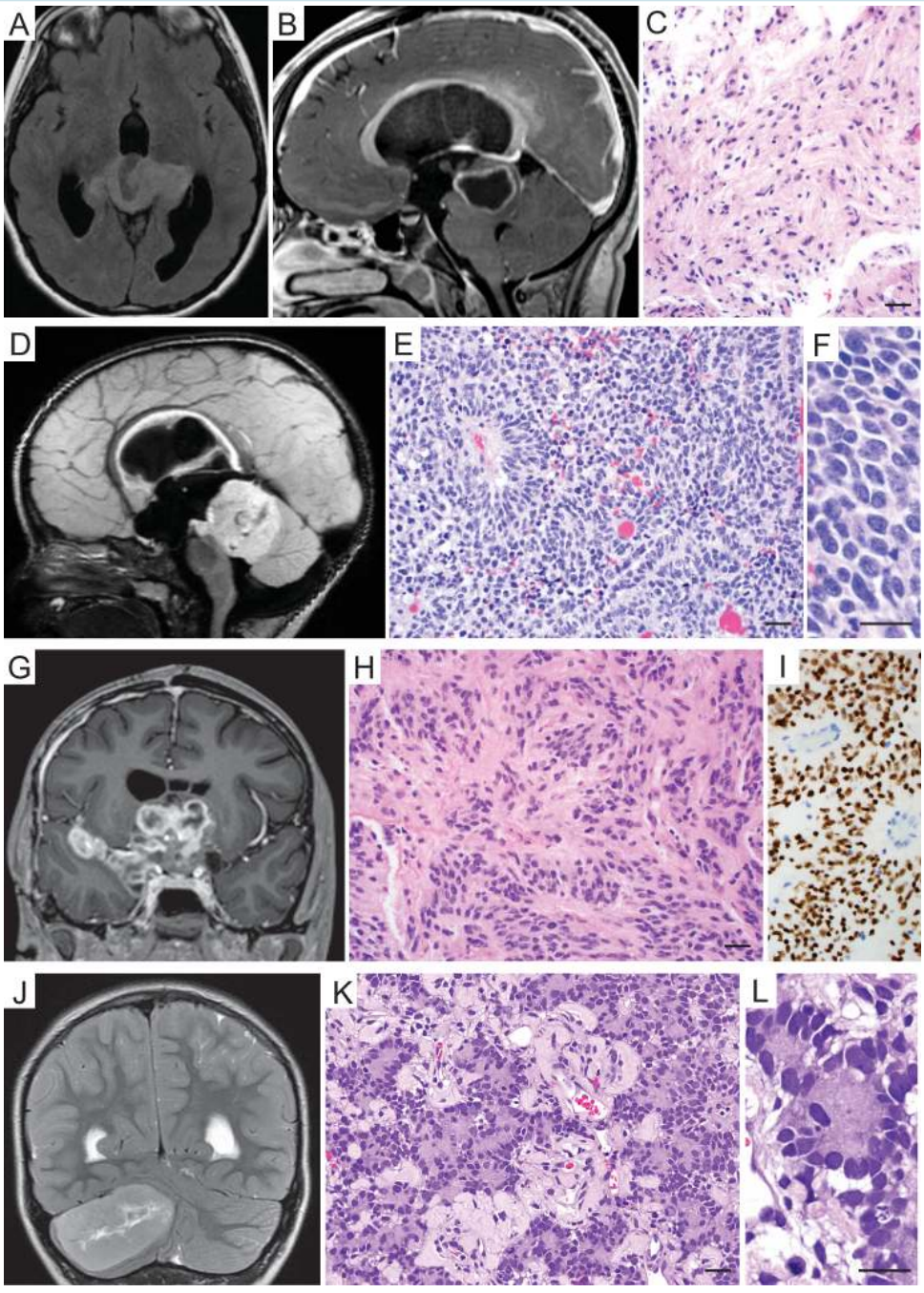


**Fig. 1** Genomic profiling improves diagnostic accuracy. (A–C) Tectal glioma in a 9-year-old boy initially diagnosed as astrocytoma of uncertain grade found to have *KIAA1549-BRAF* fusion leading to amended diagnosis of pilocytic astrocytoma, WHO grade I. (A) Axial T2-weighted FLAIR MR image revealing a tectal mass with extension into bilateral thalami. (B) Sagittal T1-weighted post-gadolinium MR image revealing peripheral enhancement and exophytic growth into the third ventricle with obstructive hydrocephalus. (C) Hematoxylin and eosin (H&E) stained section of the tumor. (D–F) Primitive neuroectodermal tumor in the midline of the posterior fossa of an 18-month-old boy initially diagnosed as medulloblastoma found to have somatic *DICER1* mutation leading to amended diagnosis of pineoblastoma. (D) Sagittal T2-weighted FLAIR MR image revealing a circumscribed solid mass centered in the midline within the region of the pineal gland causing compression of the subjacent cerebellar vermis. (E–F) H&E stained sections of the tumor. (G–I) Suprasellar mass with cerebrospinal dissemination in an 11-year-old boy initially diagnosed as ependymoma found to have *FGFR1* mutation leading to amended diagnosis of high-grade glioma. (G) Coronal T1-weighted post-gadolinium MR image revealing a complex, solid, and cystic mass in the suprasellar space. (H) H&E stained section of the tumor. (I) Immunohistochemistry showing diffuse strong staining for OLIG2 in tumor cells. (J–L) High-grade neoplasm in the cerebellum of a 4-year-old girl initially diagnosed as medulloblastoma found to have internal tandem duplication within exon 15 of *BCOR* leading to amended diagnosis of CNS high-grade neuroepithelial tumor with *BCOR* alteration. (J) Coronal T2-weighted MR image. (K–L) H&E stained sections of the tumor. Sequencing reads containing the *BCOR* internal tandem duplication are shown in Supplementary Fig. 3. Scale bar, 20 μm.

**Table 2** Relevant patient and family history in children with pathogenic germline mutations

| Patient | Sex | Age | Pathologic Diagnosis | Germline | LOH in Tumor | Other Patient Hx | Significant Family Hx (# of affected members) |
|---|---|---|---|---|---|---|---|
| 3 | F | 2 | Medulloblastoma | BRCA2 fs + fs (biallelic) | N/A | Fanconi anemia | Siblings: neuroblastoma (x1), medulloblastoma + Wilm's tumor (x1) |
| 4 | M | 5 | Medulloblastoma | PALB2 non | yes | None | Maternal lineage: breast ca (x1); Paternal lineage: breast ca (x1), liver ca (x2); Father negative for PALB2 mutation |
| 5 | M | 2 | Medulloblastoma | SUFU fs | yes | None | Maternal lineage: glioblastoma (x1) |
| 7 | M | 9 | Medulloblastoma | TP53 sub | yes | None | None |
| 9 | M | 3 | Choroid plexus carcinoma | TP53 sub, MSH6 fs | TP53 yes MSH6 no | None | None; Parents and sibling negative for TP53 mutation; Father positive for MSH6 mutation |
| 13 | M | 4 | Glioblastoma | MUTYH non | no | None | None |
| 18 | M | 10 | Glioblastoma | PMS2 non + del (biallelic) | N/A | Café-au-lait macules | Paternal lineage: café-au-lait macules (x2) |
| 19 | F | 7 | High-grade astrocytoma | TP53 sub | yes | None | Maternal lineage: early-onset breast ca (x2) |
| 20 | M | 15 | High-grade astrocytoma | MUTYH splice | yes | Medulloblastoma at age 5 | None |
| 23 | M | 12 | Diffuse astrocytoma | ERCC2 splice | no | None | None |
| 30 | F | 5 | Uveal ganglioneuroma | PTEN non | yes | Autism, macrocephaly, vascular malformations (brain, arm, foot) | Maternal lineage: early-onset uterine cancer (x4) |

**Abbreviations:** hx, history; sub, missense mutation; non, nonsense mutation; fs, frameshift mutation; splice, splice site mutation; LOH, loss of heterozygosity; del, deletion; ca, cancer

significant for early-onset uterine cancer in multiple individuals in the maternal lineage. The family has sought genetic counseling and initiated the recommended cancer screening given their newly identified tumor predisposition syndrome. To our knowledge, uveal ganglioneuroma has not been previously linked with Cowden syndrome.[16]

## Identification of Potentially Targetable Alterations

One or more genetic alterations potentially targetable by currently available therapies were identified in 19 patients (61%), listed in Table 3. The most frequently targetable mutations were activating *PIK3CA* missense mutations in high-grade gliomas known to increase sensitivity to mammalian target of rapamycin (mTOR) inhibitors such as everolimus, and amplification and/or activating missense mutations of *PDGFRA* in high-grade gliomas known to increase sensitivity to kinase inhibitors such as dasatinib.[17] Other potentially actionable alterations included inactivating *PTCH1* mutations in medulloblastomas known to increase sensitivity to Smoothened (SMO) inhibitors such as vismodegib; p.K27M missense mutation in *H3F3A* in diffuse midline gliomas that reportedly increases sensitivity to the histone deacetylase inhibitor panobinostat; and *KIAA1549-BRAF* fusion in pilocytic astrocytomas known to increase sensitivity to inhibitors of mitogen-activated protein kinase kinase (MEK) such as trametinib.[17]

Several patients have initiated treatment with these targeted therapeutics, as part of clinical trials or through off-label prescription. Patient outcomes are being evaluated and will be reported in a follow-up study. Representative examples of patients whose tumors were identified to harbor potentially targetable alterations are highlighted in Supplementary Fig. 5.

Additionally, 3 patients had glioblastomas with high somatic mutational burden consistent with hypermutation, which has been shown to predict therapeutic benefit from programmed cell death protein 1 (PD-1) blockade (eg, nivolumab).[18] One such case of exceptional interest (patient 18) is a 10-year-old boy with multiple café-au-lait macules but no other stigmata or family history consistent with neurofibromatosis. He was found to have a heterogeneously enhancing mass in the right parieto-occipital lobe, with pathology diagnostic of glioblastoma, WHO grade IV (Supplementary Fig. 6A–B). Genomic profiling revealed that the tumor had an exceptionally high mutational burden with greater than 700 somatic nonsynonymous mutations identified in the 510 genes targeted for sequencing, including mutations in several genes known to be important in gliomagenesis such as *TP53*, *PTEN*, *ATRX*, *NF1*, and *SETD2*. No pathogenic germline alterations were identified, although of note *PMS2* is not targeted for sequencing on the UCSF500 Cancer Gene Panel due to the presence of a pseudogene that interferes with

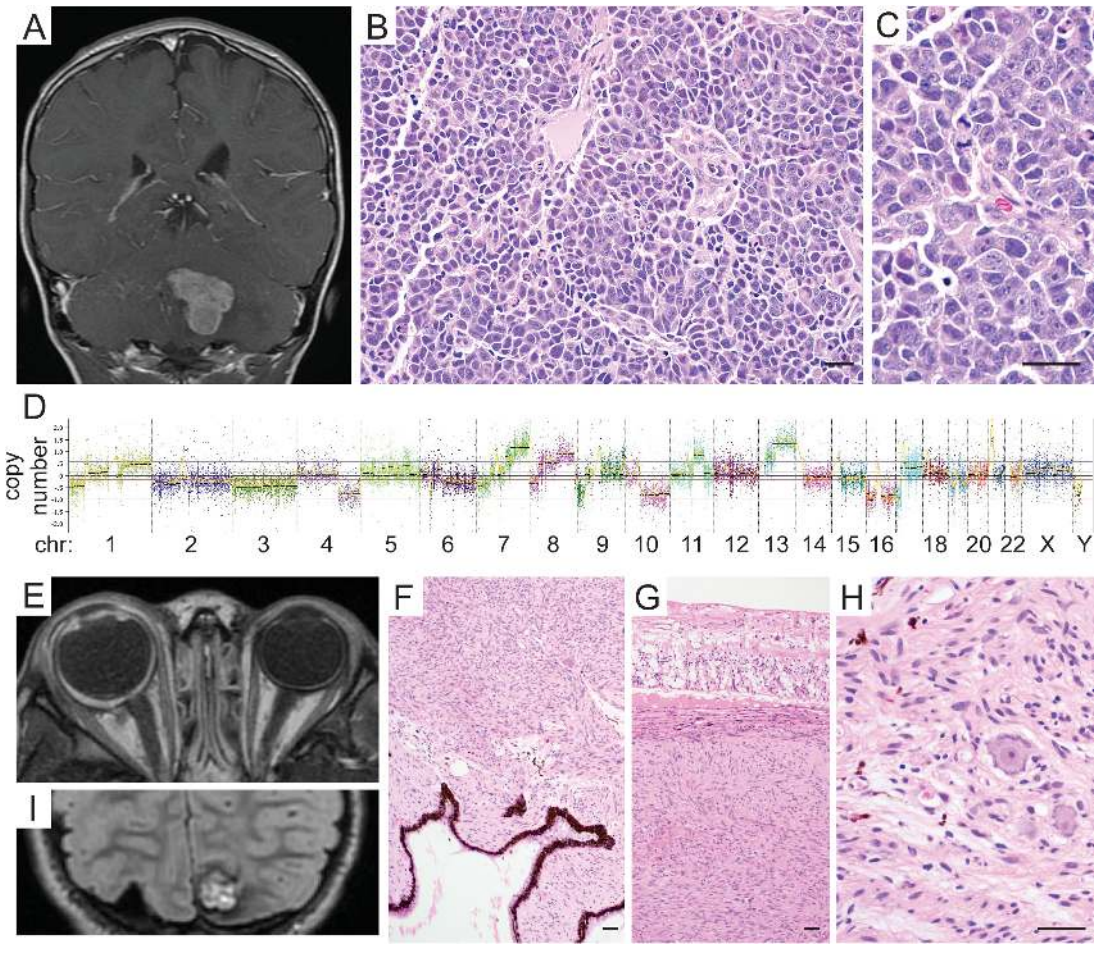


**Fig. 2** Genomic profiling identifies novel pathogenic germline mutations. (A–D) Medulloblastoma with anaplastic/large cell histologic features in a 5-year-old boy found to have monoallelic germline *PALB2* nonsense mutation with loss of heterozygosity in the tumor. (A) Coronal T1-weighted post-gadolinium MR image revealing an enhancing multinodular mass centered in the fourth ventricle and left cerebellar hemisphere. (B–C) Hematoxylin and eosin (H&E) stained sections of the tumor. (D) Genome-wide copy number plot of the tumor showing numerous chromosomal gains and losses, typical of tumors with defects in homologous recombination. (E–I) Uveal ganglioneuroma and cerebral cavernous malformation in a 5-year-old girl found to have germline *PTEN* mutation with loss of heterozygosity in the tumor. (E) Axial T1-weighted MR image of the orbits revealing diffuse thickening of the uveal tract in the right globe. (F–H) H&E stained sections of the tumor showing a spindle cell neoplasm diffusely expanding the uveal tract including the ciliary body (F) and causing retinal atrophy and detachment (G). Large dysmorphic ganglion cells were admixed among the neoplastic spindle cells, diagnostic of ganglioneuroma (H). (I) Coronal T2-weighted FLAIR MR image revealing a cavernous malformation in the left occipital lobe. Scale bar, 20 μm.

sequence alignment. Subsequent immunohistochemistry for mismatch repair proteins yielded intact expression of MLH1, MSH2, and MSH6, but no staining for PMS2 in tumor cells or nonneoplastic endothelial cells and lymphocytes (Supplementary Fig. 6C–F). Sanger sequencing of the *PMS2* gene was performed on peripheral blood, revealing compound heterozygous mutations—a nonsense mutation and intragenic deletion of exon 4. The patient was diagnosed with constitutional mismatch repair deficiency (CMMRD) syndrome (OMIM #276300), and the family is currently being evaluated by medical genetics. Following completion of radiation therapy, the patient will begin immune checkpoint therapy with nivolumab, an agent that was recently shown to have remarkable activity in children with CMMRD syndrome.[19]

## Identification of Novel Pathogenic Alterations

In addition to highlighting known genetic drivers in pediatric neuro-oncology patients, this targeted sequencing approach has identified novel likely pathogenic alterations. The first example is a 12-year-old boy (patient 21) with DIPG lacking histone H3 mutation (Fig. 3A–C), an alteration that defines the vast majority of these tumors. Instead, genomic profiling revealed a somatic nonsense mutation in *ASXL1*, which encodes an epigenetic regulator frequently mutated in pediatric acute myeloid leukemias.[20]

Patient 25 is a 12-year-old boy with a low-grade astrocytic neoplasm in the left temporal lobe with a differential diagnosis after pathologic workup that included ganglioglioma and diffuse astrocytoma (Fig. 3D–F). Genomic profiling revealed a single somatic alteration in the tumor—a small in-frame

**Table 3** Potentially targetable genetic alterations identified

| Genetic Alteration | Targeted Agent | Tumor Type | # of Patients |
|---|---|---|---|
| PIK3CA sub | mTOR inhibitor | Infiltrative astrocytoma | 3 |
| hypermutation | PD-1 inhibitor | Glioblastoma | 3 |
| PDGFRA amp or sub | dasatinib | Glioblastoma | 3 |
| KIAA1549-BRAF fusion | MEK inhibitor | Pilocytic astrocytoma | 2 |
| PTCH1 inactivation | SMO inhibitor | Medulloblastoma, nodular/desmoplastic | 2 |
| FGFR1 sub or kinase domain dup | kinase inhibitor | Low-grade glioma | 2 |
| H3F3A p.K27M | panobinostat | Diffuse midline glioma | 2 |
| AKT3 amp | mTOR inhibitor | Glioblastoma | 1 |
| MAP2K1 exon 2 small in-frame del | MEK inhibitor | Low-grade astrocytic neoplasm | 1 |
| ATG7-RAF1 fusion | MEK inhibitor | Pleomorphic xanthoastrocytoma | 1 |
| CDK4 amp | palbociclib | Glioblastoma | 1 |
| SMARCB1 del | EZH2 inhibitor | Chordoma | 1 |
| PALB2 inactivation | PARP inhibitor | Medulloblastoma | 1 |

**Abbreviations:** sub, missense mutation; amp, amplification; dup, duplication; del, deletion; EZH2, enhancer of zeste homolog 2.

deletion within exon 2 of *MAP2K1* (Fig. 3K). Similar small in-frame deletions within exon 2 of *MAP2K1* were recently reported in most Langerhans cell histiocytosis cases lacking *BRAF* p.V600E mutation, where it functions as an alternate mechanism of MAP kinase pathway activation.[21,22] Given the unresectable nature of this patient's tumor and medically refractory seizures, targeted therapy with the MEK inhibitor trametinib is being considered.

A final example is patient 29, a 19-year-old man with recurrent pleomorphic xanthoastrocytoma with anaplastic features in the left parietal lobe (Fig. 3G–J) that was found to be *BRAF* wild-type by Sanger sequencing. He underwent initial resection of pleomorphic xanthoastrocytoma without anaplasia at 17 years of age and was followed with serial imaging studies but no adjuvant therapy. Genomic profiling of the recurrent tumor revealed a novel *ATG7-RAF1* fusion (Fig. 3L), as well as homozygous deletion of *CDKN2A*. The identified fusion is predicted to result in an in-frame fusion transcript between exons 1–18 of *ATG7* and exons 8–17 of *RAF1* encoding the serine/threonine kinase domain. *RAF1* fusions have not previously been identified in pleomorphic xanthoastrocytomas, although *RAF1* gene fusions have been described in other tumor types, including melanoma and papillary thyroid cancer.[23]

## Discussion

Our experience at a Northern California tertiary medical center illustrates that targeted genomic profiling on both tumor and matched normal tissue at time of initial diagnosis or upon tumor recurrence is feasible and can have significant impact on diagnosis, identification of unsuspected germline mutations, and detection of potentially targetable mutations in the pediatric brain tumor population. Among our cohort of 31 pediatric neuro-oncology patients, 19% had pathologic diagnosis amended after testing, 35% were found to harbor a pathogenic germline mutation, and 61% had potentially targetable genetic alterations identified. As this cohort is small and contains a large fraction of high-grade and recurrent tumors, the exact frequencies of cases with pathogenic germline alterations is likely an over-representation of all pediatric neuro-oncology patients. Nonetheless, our findings highlight the need to consider cancer-predisposing germline mutations in this population even without notable family history and demonstrate the utility of up-front genetic sequencing in terms of treatment decision making and family counseling. Our experience also demonstrates that a significant fraction of pediatric neuro-oncology patients harbor potentially actionable somatic alterations, although limitations of targeted therapy such as penetration of the blood–brain barrier and acquired resistance mechanisms must be recognized.

Additionally, our findings show that a targeted capture-based sequencing assay can help to clarify diagnosis in pediatric brain tumors, which are often challenging to accurately classify. Other recent studies have shown that molecular profiling using genome-wide DNA methylation arrays can be a reliable and useful tool for aiding diagnostic classification of pediatric brain tumors.[13] However, the utility of DNA methylation profiling as a solitary tool is limited in that it does not allow assessment of germline alterations, somatic single nucleotide variants, or gene fusions. In select cases, there may be advantages of performing both DNA methylation profiling and targeted sequencing.

Noteworthy among our findings is the identification of novel tumor-predisposing germline alterations, including truncating *MUTYH* mutations in children with diffuse midline gliomas, *PTEN* mutation in a child with uveal gangli-oneuroma, and monoallelic *PALB2* mutation in a child with medulloblastoma. It remains unclear at present what the contribution of these germline alterations are in all children with these tumor types, but we speculate that future studies will indeed confirm a role of *MUTYH* and *PALB2* in pediatric gliomas and medulloblastomas. Another novel finding was the

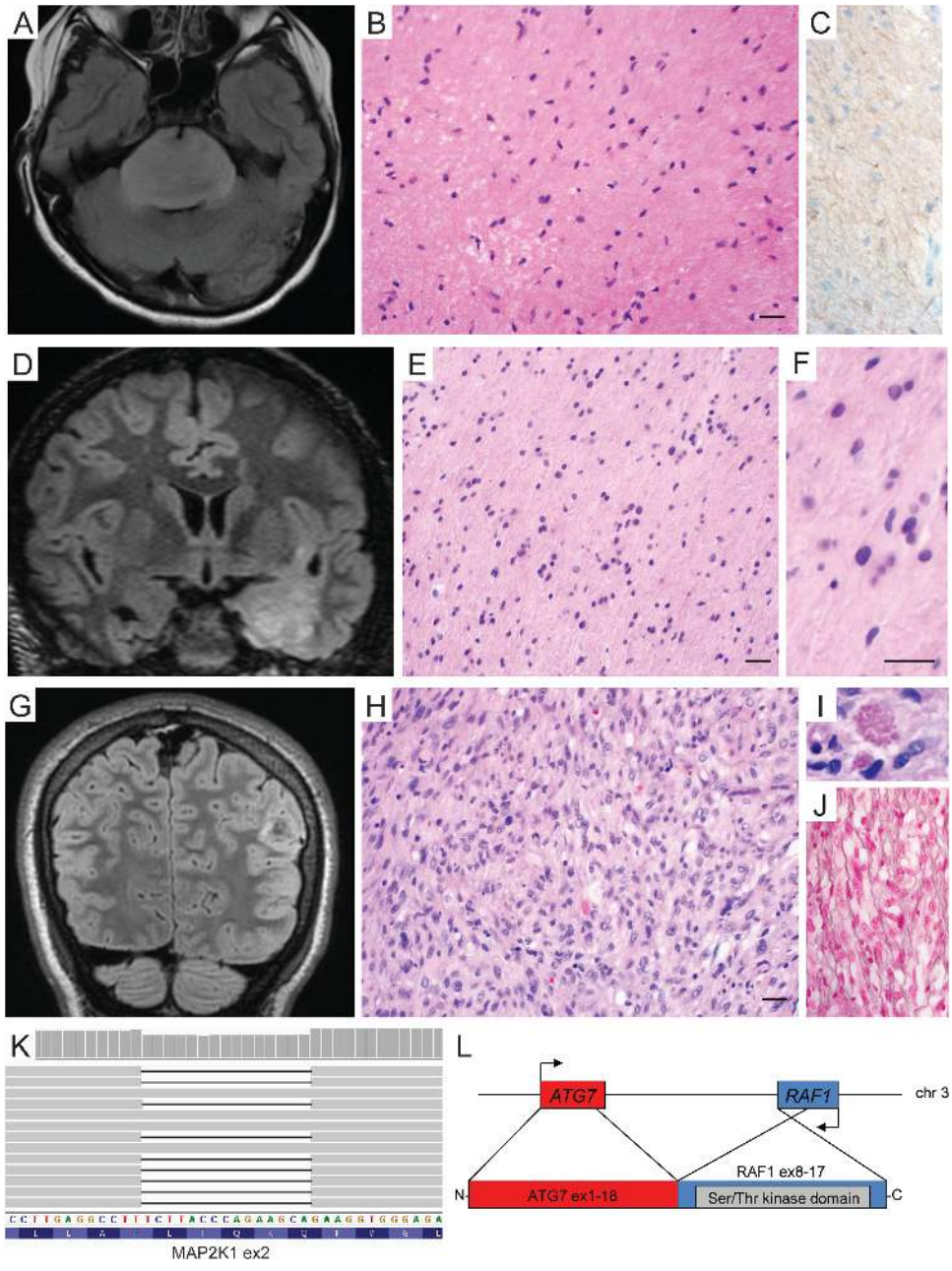


**Fig. 3** Genomic profiling identifies novel likely pathogenic alterations. (A–C) Diffuse intrinsic pontine glioma in a 12-year-old boy lacking histone H3 mutation found to have a somatic inactivating mutation in *ASXL1*. (A) Axial T2-weighted FLAIR MR image. (B) Hematoxylin and eosin (H&E) stained section of the tumor showing an infiltrating astrocytoma without high-grade features. (C) Immunohistochemistry showing absence of staining for histone H3-K27M mutant protein. (D–G, K) Low-grade astrocytic neoplasm in a 12-year-old boy found to have small in-frame deletion within exon 2 of *MAP2K1*. (D) Coronal T2-weighted FLAIR MR image showing an ill-defined, expansile mass in the left medial temporal lobe. (E–F) H&E stained sections showing a low-grade astrocytic neoplasm with densely fibrillary background. (K) Sequencing reads for the tumor mapping to exon 2 of *MAP2K1* with many containing an in-frame 15 bp deletion. (G–J, L) Recurrent pleomorphic xanthoastrocytoma with anaplastic features in a 19-year-old man lacking *BRAF* mutation found to have *ATG7-RAF1* fusion. (G) Coronal T2-weighted FLAIR MR image showing a circumscribed mass in the superficial cortex of the left parietal lobe. (H) H&E stained section showing a solid neoplasm of pleomorphic astrocytes. (I) Periodic acid–Schiff stain showing one of the many eosinophilic granular bodies in the tumor. (J) Laidlaw reticulin stain demonstrating intercellular basement membrane deposition by the neoplastic astrocytes. (L) Genetic diagram of the *ATG7* and *RAF1* loci on chromosome 3, along with the inv(3)(p25.3;p25.2) identified in the tumor resulting in production of an in-frame fusion between exons 1–18 of *ATG7* and exons 8–17 of *RAF1* encoding the serine/threonine kinase domain. Scale bar, 20 µm.

identification of *IDH1* p.R132H mutation in 2 young children with diffuse astrocytomas (patients 23 and 24), an alteration that was previously known to occur only in diffuse gliomas of older adolescents and adults.[24] Lastly, we demonstrate the utility of using a sequencing panel that covers a wide spectrum of cancer-associated genes, including those recurrently altered in non-CNS tumors, which enabled the identification of multiple novel likely pathogenic alterations in our cohort. We anticipate that these novel alterations (eg, *MAP2K1* small in-frame deletion in a low-grade astrocytic neoplasm) will prove to be recurrent mutations in pediatric brain tumors as genomic profiling continues in this population.

Moving forward, we aim to perform this genomic profiling on all pediatric brain tumor patients at our institution at time of diagnosis, with the goals of improving diagnostic accuracy, identifying therapeutically actionable alterations, offering appropriate guidance to families of patients with previously unknown germline mutations, and ultimately improving outcomes for affected children.

## Supplementary Material

Supplementary material is available at *Neuro-Oncology* online.


## Funding

No external funding was used to directly support this study.

## Acknowledgments

C.N.K. is supported by NIH T32 grant(CA128583), Alex's Lemonade Stand Foundation's Pediatric Developmental Therapeutics Center of Excellence at UCSF (A120729) and UCSF-CTSI Strategic Opportunities Support Program (A119683). S.M. is supported by the NIH National Center for Advancing Translational Sciences through UCSF-CTSI (KL2TR000143). T.N. is supported by the Pediatric Brain Tumor Foundation, Frank A. Campini Foundation, and the National Cancer Institute (P50 CA097257). D.A.S. is supported by NIH Director's Early Independence Award (DP5 OD021403) and Career Development Award from the UCSF Brain Tumor SPORE (P50 CA097257).

**Conflict of interest statement.** None for all contributing authors.


## References


1. Broniscer A, Gajjar A. Supratentorial high-grade astrocytoma and diffuse brainstem glioma: two challenges for the pediatric oncologist. *Oncologist*. 2004;9(2):197–206.
2. Northcott PA, Pfister SM, Jones DT. Next-generation (epi)genetic drivers of childhood brain tumours and the outlook for targeted therapies. *Lancet Oncol*. 2015;16(6):e293–e302.
3. Nikiforova MN, Wald AI, Melan MA, et al. Targeted next-generation sequencing panel (GlioSeq) provides comprehensive genetic profiling of central nervous system tumors. *Neuro Oncol*. 2016;18(3):379–387.
4. Sahm F, Schrimpf D, Jones DT, et al. Next-generation sequencing in routine brain tumor diagnostics enables an integrated diagnosis and identifies actionable targets. *Acta Neuropathol*. 2016;131(6):903–910.
5. Hoffman LM, Salloum R, Fouladi M. Molecular biology of pediatric brain tumors and impact on novel therapies. *Curr Neurol Neurosci Rep*. 2015;15(4):10.
6. Northcott PA, Korshunov A, Witt H, et al. Medulloblastoma comprises four distinct molecular variants. *J Clin Oncol*. 2011;29(11):1408–1414.
7. Samkari A, White JC, Packer RJ. Medulloblastoma: toward biologically based management. *Semin Pediatr Neurol*. 2015;22(1):6–13.
8. Zhang J, Walsh MF, Wu G, et al. Germline mutations in predisposition genes in pediatric cancer. *N Engl J Med*. 2015;373(24):2336–2346.
9. de Kock L, Sabbaghian N, Druker H, et al. Germ-line and somatic DICER1 mutations in pineoblastoma. *Acta Neuropathol*. 2014;128(4):583–595.
10. Raleigh DR, Solomon DA, Lloyd SA, et al. Histopathologic review of pineal parenchymal tumors identifies novel morphologic subtypes and prognostic factors for outcome. *Neuro Oncol*. DOI:10.1093/neuonc/now105
11. Jones DT, Hutter B, Jäger N, et al. International Cancer Genome Consortium PedBrain Tumor Project. Recurrent somatic alterations of FGFR1 and NTRK2 in pilocytic astrocytoma. *Nat Genet*. 2013;45(8):927–932.
12. Qaddoumi I, Orisme W, Wen J, et al. Genetic alterations in uncommon low-grade neuroepithelial tumors: BRAF, FGFR1, and MYB mutations occur at high frequency and align with morphology. *Acta Neuropathol*. 2016;131(6):833–845.
13. Sturm D, Orr BA, Toprak UH, et al. New brain tumor entities emerge from molecular classification of CNS-PNETs. *Cell*. 2016;164(5):1060–1072.
14. Kline CN, Joseph NM, Grenert JP, et al. Inactivating MUTYH germline mutations in pediatric patients with high-grade midline gliomas. *Neuro Oncol*. 2016;18(5):752–753.
15. Reid S, Schindler D, Hanenberg H, et al. Biallelic mutations in PALB2 cause Fanconi anemia subtype FA-N and predispose to childhood cancer. *Nat Genet*. 2007;39(2):162–164.
16. DeParis SW, Bloomer M, Han Y, et al. Uveal ganglioneuroma due to germline *PTEN* mutation (Cowden syndrome) presenting as unilateral infantile glaucoma. *Ocul Oncol Pathol*. In press.
17. Garcia MA, Solomon DA, Haas-Kogan DA. Exploiting molecular biology for diagnosis and targeted management of pediatric low-grade gliomas. *Future Oncol*. 2016;12(12):1493–1506.
18. Le DT, Uram JN, Wang H, et al. PD-1 blockade in tumors with mismatch-repair deficiency. *N Engl J Med*. 2015;372(26):2509–2520.
19. Bouffet E, Larouche V, Campbell BB, et al. Immune checkpoint inhibition for hypermutant glioblastoma multiforme resulting from germline biallelic mismatch repair deficiency. *J Clin Oncol*. 2016;34(19):2206–2211.
20. Huether R, Dong L, Chen X, et al. The landscape of somatic mutations in epigenetic regulators across 1,000 paediatric cancer genomes. *Nat Commun*. 2014;5:3630.
21. Brown NA, Furtado LV, Betz BL, et al. High prevalence of somatic MAP2K1 mutations in BRAF V600E-negative Langerhans cell histiocytosis. *Blood*. 2014;124(10):1655–1658.
22. Chakraborty R, Hampton OA, Shen X, et al. Mutually exclusive recurrent somatic mutations in MAP2K1 and BRAF support a central role for ERK activation in LCH pathogenesis. *Blood*. 2014;124(19):3007–3015.
23. Stransky N, Cerami E, Schalm S, et al. The landscape of kinase fusions in cancer. *Nat Commun*. 2014;5:4846.
24. Ferris SP, Goode B, Joseph NM, et al. IDH1 mutation can be present in diffuse astrocytomas and giant cell glioblastomas of young children under 10 years of age. *Acta Neuropathol*. 2016;132(1):153–155.